Local Dynamics and Molecular Origin of Polymer Network−Water Interactions as Studied by Broadband Dielectric Relaxation Spectroscopy, FTIR, and Molecular Simulations

Jovan Mijović* and Hua Zhang

Department of Chemical Engineering and Chemistry and The Herman F. Mark Polymer Research Institute, Polytechnic University, Six Metrotech Center, Brooklyn, New York 11201

Received October 9, 2002; Revised Manuscript Received December 6, 2002

ABSTRACT: An investigation was carried out of the molecular interactions and local relaxation dynamics in glassy polymer networks exposed to moisture. Stoichiometric and off-stoichiometric mixtures of the diglycidyl ether of bisphenol A (DGEBA) and diethylene triamine (DETA) were prepared, cured, and investigated. The physical and the chemical nature of the interactions between the network and the absorbed moisture were studied by broadband dielectric relaxation spectroscopy (DRS), Fourier transform near-infrared (FT-NIR) spectroscopy, and molecular simulations. Dry networks are characterized by two Arrhenius-like local relaxations: the β process, associated with hydroxyl groups, and the γ process, associated with primary and secondary amine, and glycidyl ether groups. Absorbed water interacts with the network and affects the dynamics of β and γ processes. FT-NIR spectra reveal the presence of three forms of water molecules, differing in the number of hydrogen atoms (0, 1, or 2) that participate in hydrogen bonds. The relative ratio of each form to the total absorbed water was calculated from the NIR data and from molecular simulations. An excellent agreement between those two techniques was observed.

I. Introduction

The effect of absorbed moisture on the molecular interactions and relaxation dynamics in polymer networks is an interesting, fundamentally important and incompletely understood problem.[1−7] The work presented herein addresses this issue by examining a glassy thermoset network exposed to moisture with the combined use of broadband dielectric relaxation spectroscopy (DRS), Fourier transform infrared spectroscopy (FTIR), and molecular simulations.

The consensus of opinion in the polymeric adhesives community, where moisture absorption assumes paramount importance, is that the chemical and physical changes on the *molecular level* during the early stage of environmental exposure (prior to the formation of voids and microcracks that lead to the degradation of joints) hold the key to the prediction of performance.[8] The vast majority of the reported studies (e.g., refs 9-20), however, have been concerned with the effect of moisture on the *macroscopic* (bulk) properties and/or the detection of delamination and loss of adhesion that occur when water eventually diffuses through the adhesive and reaches the adhesive/adherend interface/interphase. Consequently, a number of fundamental questions about the *molecular-level* events in glassy adhesives remain unanswered. In what form (single molecules, dimers, trimers, hydrogen-bonding complexes) does the absorbed water reside in the adhesive? How does water interact with the host matrix, and what effect does it have on the local dynamics? How are dynamics affected by the temperature, pressure, and relative humidity of the environment? The fundamental knowledge gained from such studies is expected to usher the way for the development of a methodology that can predict the course of subsequent degradation and anticipate failure of those materials.

The paucity of information about the effect of absorbed moisture on the local relaxation dynamics in glassy polymers is caused to a large measure by the short time scale of these processes (often as fast as a few picoseconds and hence not easily measured). Of the few experimental techniques operable at high frequency and adaptable to the adhesive joint configuration, dielectric relaxation spectroscopy (DRS) is rapidly becoming a dominant tool,[21] owing to its unparalleled frequency range (up to 16 decades). The fundamental aspects of DRS, theoretical and experimental, will not be discussed here, and the interested reader is referred to a number of excellent sources.[22−24] Of course, the interpretation of molecular dynamics obtained from DRS can be greatly aided with the use of a complementary technique capable of providing specific information about the chemical state of the matter. Among those techniques, FTIR represents the most attractive choice: fundamentally—because of the unmatched wealth of information about the chemical state of the matter contained in the infrared spectrum—and practically—because of the adaptability of near-FTIR (NIR) to remote (fiber optic) in situ real-time applications and the possibility of using NIR for nondestructive inspection (NDI). A comparison of DRS and NIR data with the results obtained from molecular simulations is of further interest.

Therefore, the principal objective of this study is a combined use of DRS, FTIR, and molecular simulations designed to afford a simultaneous evaluation of physical and chemical changes at the molecular level in glassy thermoset networks exposed to moisture. Naturally, the implications of this work extend beyond thermoset adhesives and are important to a range of topics related

* To whom correspondence should be addressed. E-mail: jmijovic@poly.edu.

10.1021/ma021568q CCC: $25.00
Published on Web 01/31/2003

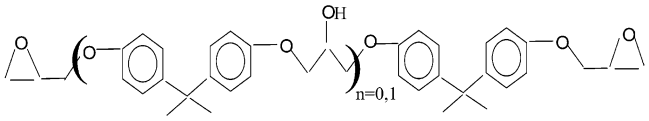

DGEBA

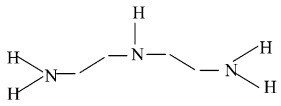

DETA

Figure 1. Chemical structures of diglycidyl ether of bisphenol A (DGEBA) and diethylenetriamine (DETA).

to water dynamics in synthetic polymers and biopolymers, in thin films and confined spaces, and in glass formers in general.

II. Experimental Section

Materials. A two-component reactive mixture composed of the diglycidyl ether of bisphenol A (DGEBA) and diethylenetriamine (DETA) was used in this study. Both chemicals were obtained from Aldrich Chemical Co. and were used as received. The chemical structures of DGEBA and DETA are given in Figure 1. The two liquid components were mixed and stirred continuously until a clear, homogeneous mixture was obtained. Both the stoichiometric and off-stoichiometric ratios were prepared and investigated. A typical cure schedule consisted of keeping the as-mixed sample for 12 h at 20 °C, followed by 90 min at 65 °C and another 90 min at 130 °C. Samples were cured between two aluminum adherends. The adherend surface was grinded and cleaned with acetone prior to the application of the resin and the bondline thickness was 100 μm. The chemical changes during cure of the reactive mixture were monitored by near-infrared (NIR) spectroscopy. The cured samples were fully reproducible (DSC and FTIR controls were run) and were subjected to identical thermal history (by heating above the T_g and then cooling) prior to the exposure to environment to minimize the effect of structural relaxation (physical aging) between different samples. Samples were then exposed to the aggressive environment at 80 °C and 98% RH. Relative humidity (RH) was maintained with a saturated $NaHSO_4$ solution. Samples were removed from the environment at selected time intervals, weighed and tested. Sample weight was recorded on a Mettler Toledo AX105 balance, with a precision range of ±0.005 mg.

Techniques. The principal experimental technique we used is broadband DRS. A brief description of our experimental facility for dielectric measurements follows; more details are given elsewhere,[25,26] and several excellent reviews of experimental methodology for dielectric measurements were recently published.[27,28] In this study we have used Novocontrol's α analyzer (3 μHz to 10 MHz) and a Hewlett-Packard 4291 B RF Impedance analyzer (1 MHz to 1.8 GHz). Both instruments are interfaced to computers via IEEE 488.2 and are connected to a heating/cooling unit (modified Novocontrol's Novocool System) equipped with a custom-made motor driven arm that can selectively insert into the Novocool cryostat chamber either the low-frequency or the high-frequency sample cell. This configuration has the advantage of providing high-precision temperature control over the entire frequency range (3 μHz to 1.8 GHz). A variety of sample cells were employed, including parallel plates, high precision extension airlines, etc.

Supporting evidence was obtained from Fourier transform infrared (FTIR) spectroscopy, using Nicolet Instrument's Magna 750 spectrometer, and differential scanning calorimetry (DSC), using Perkin-Elmer model 7 DSC, at a heating rate of 10 °C/min.

Simulations were conducted with Materials Studio (Accelrys Inc.) software according to the following procedure. First, a network consisting of 25 DGEBA and 10 DETA molecules was built using a polymer building function. Then, an amorphous cell composed of the DGEBA−DETA network and a select number of water molecules was constructed with the Amorphous Cell module, the experimentally obtained value for the network density (ρ = 1.165 g/cm^3) was used. The potential energy of the amorphous cell was then minimized until the root-mean square derivative was 1.0 (kcal/mol)/Å or less. Upon the completion of minimization, the amorphous cell was first equilibrated at 353 K (moisture absorption temperature) for 30 ps and then at 293 K for 50 ps. The constant temperature, constant density condition (*NVT* ensemble) was used. The final structure was then recorded and studied. The interatomic interactions were modeled with the COMPASS[29] (condensed-phase optimized molecular potentials for atomistic simulation studies) force field. The energy expression of COMPASS comprises a combination of valence terms, a Coulombic term for the electrostatic interactions and a Lennard-Jones 9−6 function for the van der Waals interactions. For calculation of the electrostatic interactions, the cell multipole method[30−32] was used; for the calculation of the van der Waals interactions, the atom-based summation method with a 9.5 Å cutoff was employed. For each select water content, 10 cells were averaged to get statistically meaningful results; at the lowest water content of 0.4%, however, 20 cells were averaged. A total of over 70 simulations were run; simulation time for one cell was about 12 CPU hours on a 1.3GHz PIV PC.

III. Results and Discussion

Dry Networks. We shall start by describing the DRS response of a dry, fully cured stoichiometric network. The temperature range covered by the DRS measurements of stoichiometric networks is from −80 to + 190 °C. Above 130 °C, we observe the segmental α process (the calorimetric T_g of the fully cured network is 120 °C) that is well described by the Havriliak−Negami (HN) functional form.[33] The HN equation is a generalization of the Cole−Cole (CC) equation, to which it reduces for b = 1, and a generalization of the Cole−Davidson (CD) equation, to which it reduces for a = 1. The average relaxation time, defined as $\tau = {}^1/_2\pi f_{max}$, where f_{max} is the frequency of maximum loss, shows the well-known Vogel−Fulcher−Tammann (VFT) temperature dependence, and the α process is thermodielectrically simple with a Kohlrausch−Williams−Watts[34] (KWW) β parameter of 0.47. Of course, we shall not be principally concerned here with the α dynamics, because our networks are utilized at temperatures well below the calorimetric T_g, where network dynamics are governed by local relaxations. In Figure 2, we show dielectric loss in the frequency domain at various temperatures below 60 °C. Two local relaxation processes are observed and termed β and γ in the order of increasing frequency at a constant temperature; a deconvoluted spectrum at −60 °C is shown in the inset of Figure 2, with solid lines representing the Cole−Cole functional form. Both β and γ processes have Arrhenius temperature dependence with activation energies of 60 and 40 kJ/mol, respectively.

A prerequisite for the study of chemophysical interactions between the network and the absorbed moisture is an understanding of the molecular origin of β and γ relaxations in the dry network. We acknowledge the ongoing debate in the literature about the nature of the β process in glass formers[35−39] and its relation to the α process[39,40] but hasten to add that we view β relaxation in our networks as a separate process in the Johari−Goldstein sense[40] below the $\alpha\beta$ splitting temperature. Earlier studies[41,42] suggested that β and γ relaxations in epoxy networks were related to the localized motions

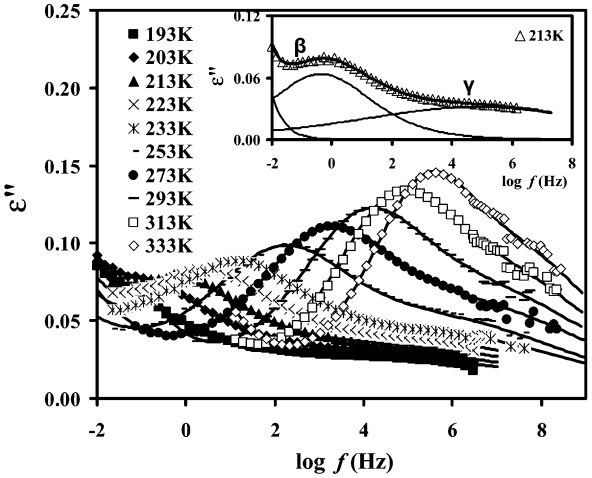

Figure 2. Dielectric loss in the frequency domain for a dry stoichiometric DGEBA−DETA network at temperatures below 60 °C. Solid lines are Cole−Cole fits. The inset shows a deconvoluted relaxation spectrum of a dry stoichiometric DGEBA−DETA network at −60 °C.

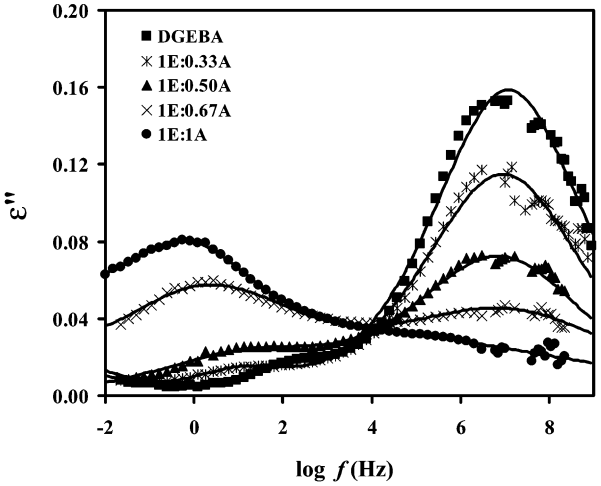

Figure 3. Dielectric loss in the frequency domain for a series of epoxy-rich DGEBA−DETA networks and neat DGEBA measured at −60 °C.

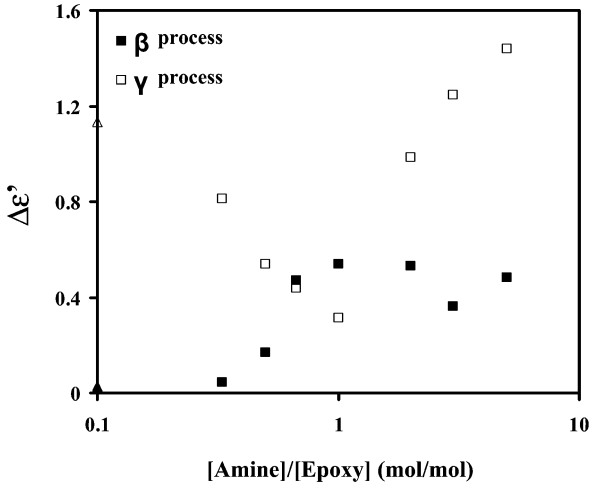

Figure 4. Dielectric relaxation strength of β and γ processes at different E:A ratios. Solid and open squares describe the β and the γ process of networks, respectively. Triangles (on the ordinate) describe β and γ processes in the neat DGEBA.

of hydroxyl groups and ether linkage of the glycidyl moiety, respectively. To verify this, we have undertaken a systematic investigation of a series of dry, cured, off-stoichiometric DGEBA−DETA formulations. By varying the stoichiometry, we were altering, in a quantitatively controlled manner, the relative ratios of four dipolar moieties (hydroxyl, ether, amine, and epoxy) in the network and observing the ensuing effect on the DRS spectra. In the discussion that follows, all formulations are defined by the epoxy (E) to amine hydrogen (A) ratio normalized with respect to one epoxy group; for example, the 1E:1A ratio denotes a stoichiometric mixture. Subscripts E and A are used in the off-stoichiometric mixtures to distinguish between the relaxation processes in epoxy rich (β_E and γ_E) and amine-rich (β_A and γ_A) formulations. No subscripts are used for relaxations in the dry stoichiometric formulation. The results obtained on the off-stoichiometric formulations proved quite revealing, as we consider the epoxy rich formulations first.

A typical example of dielectric loss in the frequency domain for several epoxy rich formulations and neat DGEBA measured at −60 °C is given in Figure 3. Measurements conducted at various temperatures between −80 and + 60 °C yielded analogous results and are not shown here. The intensity and the dielectric relaxation strength, $\Delta_{\beta E}$, defined as $\Delta\epsilon_{\beta E} = \epsilon_0 - \epsilon_\infty$ of the β_E process (seen at lower frequency in Figure 3) decrease with an increase in the E:A ratio. This finding is readily rationalized: hydroxyl groups, which are at the heart of the β process, are the product of epoxy−amine reactions and their concentration decreases with an increase in the E:A ratio. A slight increase in the average relaxation time (shift to lower frequency) of the β_E process with increasing E:A ratio is attributed to the difference in the local environment (different chemical composition as a result of different epoxy/hydroxyl ratio, different cross-linking density, different departure from T_g, etc.). As a point of information we note that the calorimetric T_g (which reflects segmental, not local motions), increases from −12, to +31, to +48, and to +120 °C with a decrease in the E:A ratio from neat DGEBA, to 1:0.33, to 1:0.5, and to 1:1.

The intensity and the dielectric relaxation strength of the γ_E process (seen at higher frequency in Figure 3) increase with increasing E:A ratio. A similar process is also seen in the neat DGEBA, and hence, the γ_E process was assigned to the relaxation of the remaining (unreacted) glycidyl groups. Especially interesting is the presence, at all temperatures, of an isosbestic point in the DRS spectra, i.e., the frequency at which the dielectric loss is independent of the composition. The presence of an isosbestic point is a signature of two relaxation processes. We also observe a shift in the isosbestic point to higher frequency by approximately one decade for every 20 °C.

We now briefly examine amine-rich formulations. The relaxation spectra of networks with E:A ratios ranging from 1:1 to 1:5 were fit with two Cole−Cole (CC) equations, and the relaxation strength of the β_A and γ_A processes ($\Delta_{\beta A}$ and $\Delta_{\gamma A}$, respectively) was calculated. Figure 4 includes the relaxation strength of β and γ processes in amine- and epoxy-rich networks. We observe that $\Delta\epsilon_\beta$ increases with increasing amount of amine when E:A ≥ 1, because of the concomitant increase in the concentration of hydroxyl groups. A further increase in the amine concentration beyond the

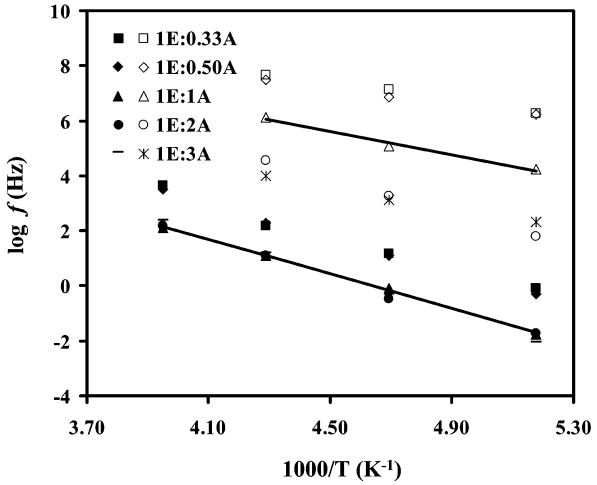

Figure 5. Frequency at maximum loss as a function of reciprocal temperature for a series of stoichiometric and off-stoichiometric networks. Solid and open symbols describe the β and the γ process, respectively.

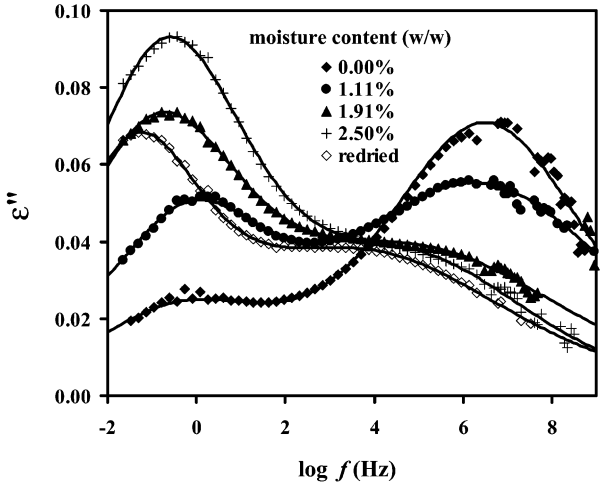

Figure 6. Dielectric loss in the frequency domain for a 1E:0.5A DGEBA−DETA network with moisture content as a parameter, measured at −80 °C.

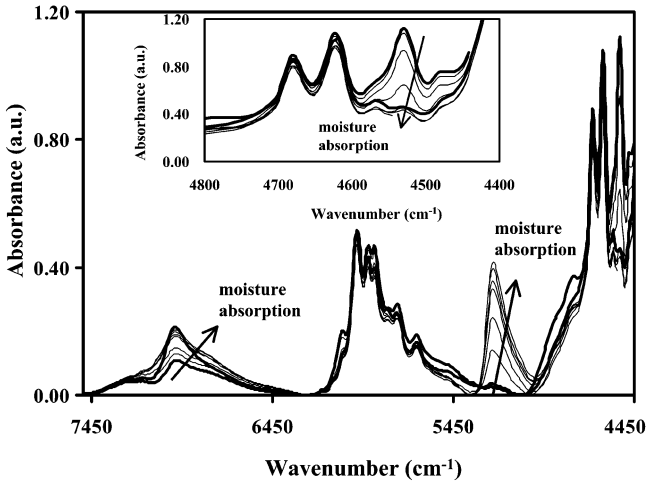

Figure 7. NIR spectra at different exposure times of a 1E:0.5A network. In the direction of the arrow, the spectra correspond to dry, 1 h, 4 h, 11 h, 24 h, 33 h, and 48 h. The two thicker curves are for dry (bottom) and for redried (middle) sample; the consumption of epoxy groups in the 4800−4400 cm^{-1} range is clearly seen in the inset.

stoichiometric ratio (i.e., when E:A < 1) has no effect on $\Delta\epsilon_\beta$.

A composite plot of frequency at maximum loss (f_{max}) as a function of reciprocal temperature for networks with different E:A ratios is shown in Figure 5. An Arrhenius temperature dependence was observed and the calculated activation energies for the β and γ processes of 60 and 40 kJ/mol, respectively, were independent of the E:A ratio.

In sum, it is safe to say that the DRS spectra of dry networks with varying stoichiometry provide further evidence that the β process is associated with hydroxyl groups while the γ process involves primary and secondary amine and ether groups.

Moist Networks. We now consider how the acquired understanding of the molecular origin of local relaxations can help us elucidate the interactions between the polymer network and the absorbed moisture. In the process of doing so, we shall examine the DRS spectra of samples of different stoichiometry, at different levels of moisture uptake, and at different measuring temperatures. The variation in stoichiometry has a profound effect on the dielectric response of moist samples, as illustrated below. The results for the epoxy-rich formulations are exemplified in Figure 6 which shows dielectric loss in the frequency domain for a 1E:0.5A formulation measured at −80 °C, with moisture content (%) as a variable. Note a systematic increase in the relaxation strength of the β_E process and a simultaneous decrease in the strength of the γ_E process. Both changes are irreversible, as clearly established by examining the spectrum of a redried sample. An explanation was sought and obtained with the aid of near-FTIR (NIR) and mid-FTIR (MIR) measurements, briefly described below. The characteristic NIR and MIR absorption bands in epoxy−amine formulations are well-documented,[43,44] and we shall omit reviewing them here. In Figure 7, we show a series of NIR spectra of a 1E:0.5A network taken at various times during moisture uptake. Note the increase in the intensity of the characteristic peaks due to absorbed water (at 5235 cm^{-1}) and hydroxyl groups (at 7000 cm^{-1}). Surprisingly, however, there is a simultaneous decrease in the intensity of epoxy absorption (at 4530 and 6000 cm^{-1}). That observation, taken together with the irreversible increase in the hydroxyl absorption band at 7000 cm^{-1} (analogous observations were made in the MIR spectra not shown here), leaves little doubt that a chemical reaction occurs between epoxy groups and water. This was intuitively unexpected, and a number of model systems were examined to provide corroborating evidence. We shall not be comprehensive here; suffice it to say that the epoxy−water reaction will take place in the presence of a tertiary amine catalyst. For example, NIR spectra of neat DGEBA in contact with water vapor at 80 °C did not change at all with exposure time in excess of 24 h, while a dramatic change (increase in hydroxyl absorption, decrease in epoxy absorption) was observed upon the addition of a small amount of tertiary amine that acts as a catalyst for the reaction between DGEBA and water. The possibility of chemical reaction between epoxy group and water is of further practical importance in the light of the frequent use of epoxy rich formulations as matrices in composite materials.

Reverting our attention to the dynamics of the β_E process in moist samples, we observed a gradual increase in the average relaxation time (see Figure 6)

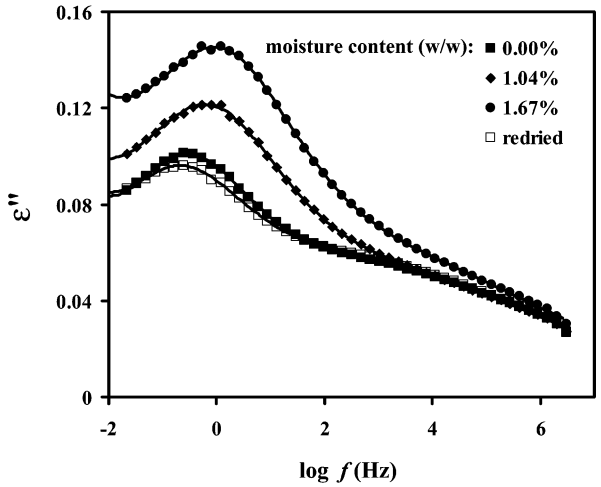

Figure 8. Dielectric loss in the frequency domain for 1E:2A DGEBA−DETA network with moisture content as a parameter, measured at −60 °C.

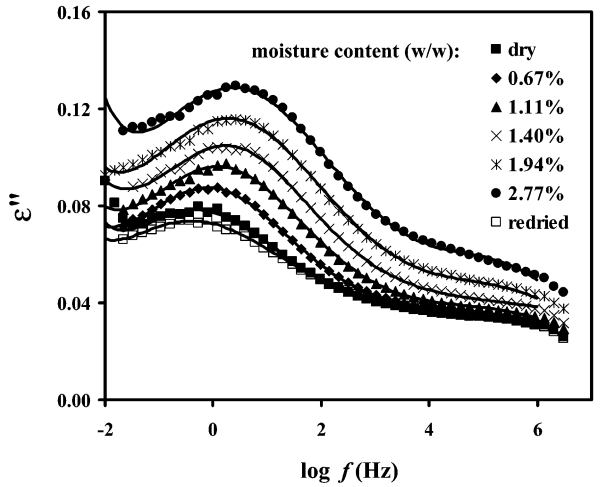

Figure 9. Dielectric loss in the frequency domain for 1E:1A DGEBA−DETA network with moisture content as a parameter, measured at −60 °C.

followed by leveling off at about 1.5% water content. A further increase in the average relaxation time for the β_E process was noted in the redried samples. Analogous trends were observed at different measuring temperatures.

The intensity and the relaxation strength of the γ_E process decrease with moisture uptake. Considering that the γ_E process comprises local relaxations of epoxy rings, the observed decrease in $\Delta\epsilon_{\gamma E}$ is in agreement with the depletion of epoxy groups due to chemical reaction during moisture uptake.

The effect of moisture on the dynamics of the amine-rich formulations is also evident in the range of β_A relaxation (Figure 8) and is attributed to the interaction between hydroxyl groups and water molecules during moisture uptake. Two interesting observations were made that stand in contrast with the epoxy rich formulations: (1) the average relaxation time for the β_A process decreases (shifts to higher frequency) with increasing moisture content, and (2) the observed increase in the intensity and the dielectric relaxation strength that accompany moisture uptake are fully reversible. This is illustrated in the dielectric spectrum of Figure 8 for a 1E:2A formulation measured at −60 °C, with moisture content (%) as a parameter. Analogous DRS results were obtained at other measuring temperatures and no changes were observed in the NIR and/or MIR spectra of dry and redried samples. The effect of absorbed moisture on the γ_A process is negligible. A possible explanation could be sought in the water−amine interactions that result in the formation of a quaternary ammonium cation and a hydroxyl anion that contribute to conductivity rather than relaxation. Some support for this hypothesis comes from the higher values of the measured conductivity and diffusion coefficient in the amine-rich networks.

We now return our attention to the stoichiometric formulation and examine in further detail the effect of absorbed moisture on the local dynamics and the molecular origin of water−network interactions. We preface the presentation and discussion of these results with two comments. First, we stress that we shall not be principally concerned with the kinetics of moisture absorption.[45−47] We limit ourselves to saying that the diffusion process is Fickian and that the calculated value of the diffusion coefficient of 4.42×10^{-8} cm^2 s^{-1} is in agreement with the literature.[48] And second, we acknowledge efforts to monitor moisture absorption in polymers by tracking dielectric permittivity at a constant frequency[6,48] but hasten to add that our DRS spectra were recorded and quantified over a wide frequency range. In Figure 9, we show dielectric loss in the frequency domain with moisture content (%) as a parameter measured at −60 °C. Again, analogous results were obtained at other measuring temperatures and are not shown here. The intensities of β and γ processes increase with moisture uptake, and the moisture absorption is fully reversible. Interestingly, the average relaxation time for the β process decreases with moisture uptake. To quantify the net effect of the absorbed water on the local dynamics, spectral subtraction was performed and the resulting difference spectra are shown in Figure 10. The two processes (β_m and γ_m) can be readily deconvoluted and fitted with two Cole−Cole functions at temperatures below −30 °C (shown in the inset of Figure 10). Subscript m is used in the text below to distinguish moist from dry (no subscript)

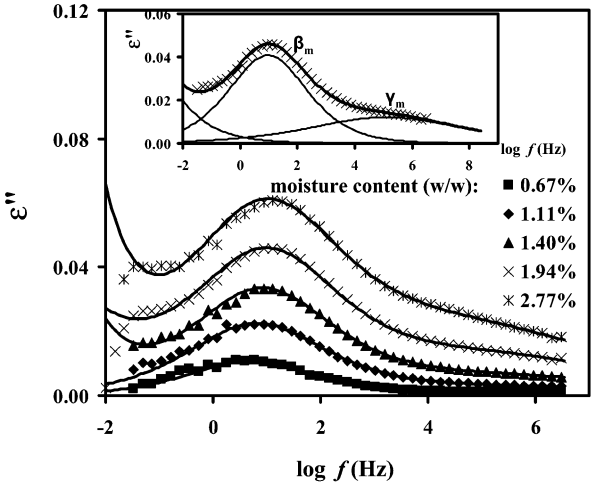

Figure 10. Difference dielectric spectra of 1E:1A DGEBA−DETA network in the frequency domain with moisture content as a parameter, measured at −60 °C. The inset shows a deconvoluted difference spectrum of 1E:1A DGEBA−DETA network with the aid of two Cole−Cole functions and a low-frequency dc conductivity dependence (with 1.94% moisture, measured at −60 °C).

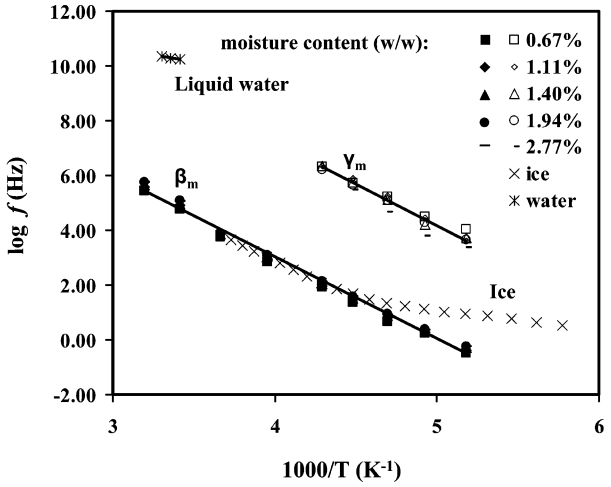

Figure 11. Frequency at maximum loss as a function of reciprocal temperature for β_m (solid symbols) and γ_m (open symbols) relaxations, with moisture content as a parameter. Also shown are the frequency at maximum loss data for ice (X) and liquid water (∗).

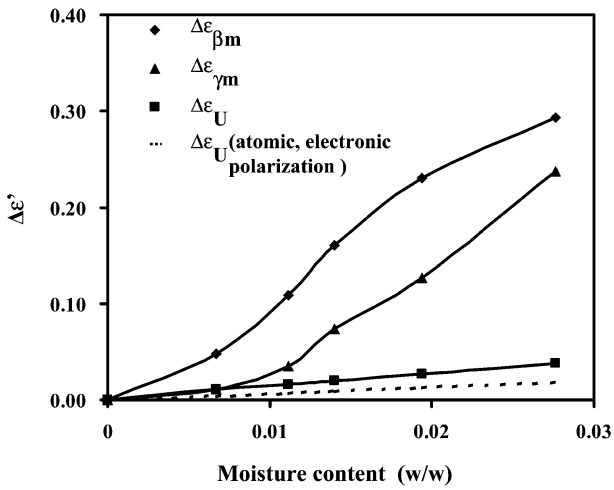

Figure 12. Dielectric relaxation strength of β_m and γ_m processes and the $\Delta\epsilon_U$ term as a function of moisture content, measured at −60 °C.

stoichiometric networks. The following equation was used to fit the data:

$$\Delta\epsilon^* = \frac{\Delta\epsilon_{\beta m}}{1 + (i\omega\tau_{\beta m})^{a_{\beta m}}} + \frac{\Delta\epsilon_{\gamma m}}{1 + (i\omega\tau_{\gamma m})^{a_{\gamma m}}} + \Delta\epsilon_U \qquad (1)$$

In eq 1, Δ is the relaxation strength, τ the relaxation time, a the Cole−Cole parameter, the subscripts βm and γm refer to the β and γ processes in the difference spectra of moist networks, and ϵ_U is the limiting high-frequency permittivity. Above −30 °C, however, deconvolution is too uncertain to be considered physically meaningful. Both β_m and γ_m relaxations have an Arrhenius temperature dependence (Figure 11) with an activation energy of ca. 58 kJ/mol.

At this point, notwithstanding the form in which water resides in the network, it is instructive to compare our results with the dynamics of (isotropically mobile) bulk liquid water[49] and ice. For that purpose, we have included in Figure 11 data for pure liquid water and ice. At 20 °C, liquid water has a dielectric loss peak at about 20 GHz,[49,50] corresponding to an average relaxation time of ca. 9 ps. This is faster than the extrapolated value for the γ_m process and many orders of magnitude faster than the β_m process. Dielectric spectra of pure ice are also very interesting; the average relaxation time for ice is commensurate with that for the β_m process between 0 and −40 °C but becomes faster below that temperature. We report the coincidence of the data for ice and moist network in the 0 to −40 °C range as a curiosity, and no further attempts were made at clarifying the molecular origin of that observation. Because bulk liquid water relaxes at much higher frequency (and water vapor at still higher frequency[51]) than the β_m or the γ_m process, the contribution (if any) from liquid water or vapor to the dielectric permittivity of moist networks ought to be contained within the $\Delta\epsilon_U$ term. Of course, that term contains the contribution from atomic and electronic polarization from all water molecules, and hence, an increase in $\Delta\epsilon_U$ with moisture would suggest an increase in the content of the isotropically mobile water (or vapor). Furthermore, since the β_m process originates from the interactions between water and hydroxyl groups and the γ_m process originates in the interactions between water and glycidyl ether groups, the relative change in the strength of these two relaxations with moisture content should provide a clue about the ratio of water hydrogen-bonded to hydroxyl and to glycidyl ether groups. Changes in the dielectric relaxation strength of β_m and γ_m processes and the $\Delta\epsilon_U$ term were calculated as a function of moisture content and plotted in Figure 12. It is immediately clear that the increase in the relaxation strength of the β_m ($\Delta\epsilon_{\beta m}$) and/or the γ_m ($\Delta\epsilon_{\gamma m}$) process is much greater than the increase in $\Delta\epsilon_U$ indicating a strong preference of the absorbed moisture for participation in the β_m and γ_m processes. The dashed line shown in Figure 12 is calculated from the following equation based upon the contribution from atomic and electronic polarization of total moisture:

$$\Delta\epsilon_U(\text{atomic, electronic polarization}) = [\epsilon_\infty(\text{ice}) - \epsilon_\infty(\text{dry resin})] \times \text{moisture content} \qquad (2)$$

The value of $\epsilon_\infty = 3.1$[52] for ice was used in the calculation. As seen in Figure 12, the measured value of $\Delta\epsilon_U$ is only slightly higher than the value calculated based on the contribution from atomic and electronic polarization; the difference between the two values of $\Delta\epsilon_U$ amounts to about 5% of the total increase in the overall dielectric relaxation strength ($\Delta\epsilon_{\beta m} + \Delta\epsilon_{\gamma m} + \Delta\epsilon_U$) due to moisture absorption. This suggests that, within the accuracy of the estimate and the measurement, the contribution of liquid (and/or vapor) water to $\Delta\epsilon_U$ is on the order of 5%, implying that the majority of absorbed water relaxes as a part of the β_m and/or the γ_m process. The finding that only about 5% of the absorbed moisture in the DGEBA−DETA network is in the form of "free water" is in contrast with the earlier reports for bis(maleimide) (BMI)[53] networks and other epoxy−amine networks.[6,48] In BMIs, however, there is a likelihood of void formation as a result of etherification reaction and the absorbed water can accumulate in those voids. In the other epoxy−amine networks studied, the calculation of "free water" was based on the value of dielectric permittivity at 1 MHz at room temperature; consequently, only the β process was considered as representative of "bound water", while the interactions that underlie the γ process were lumped under "free water", yielding the high reported value.

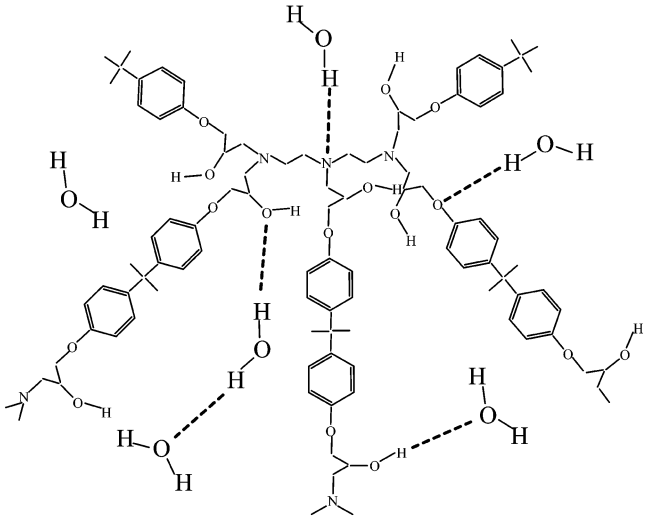

Figure 13. Schematic of a network fragment with absorbed water molecules; possible water−network interactions are indicated by dashed lines.

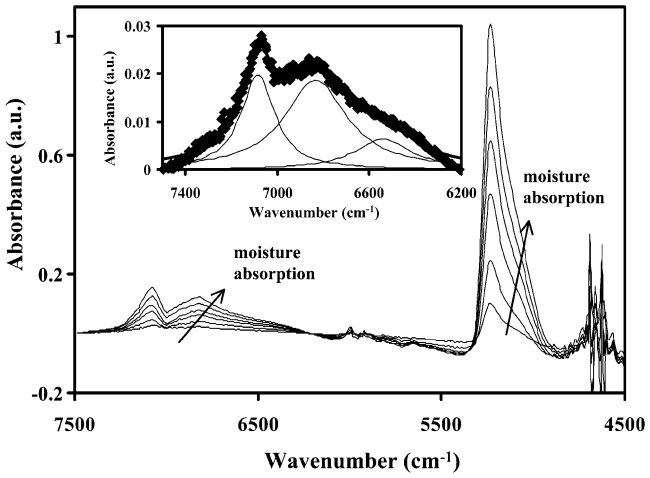

Figure 14. NIR difference spectra of 1E:1A DGEBA−DETA network with different moisture content. In the direction of the arrow, the moisture content (w/w) is: 0.46%, 1.02%, 1.58%, 2.03%, 2.41%, 2.69%. The inset shows a deconvoluted difference spectrum (7500−6200 cm^{-1}) of a 1E:1A DGEBA−DETA network with 0.46% moisture content.

We acknowledge here the possibility that the change of free volume fluctuations and physical aging may affect the relaxation strength of the β process ($\Delta\epsilon_\beta$). However, the change of free volume fluctuations induced by additives was reported to decrease $\Delta\epsilon_\beta$ in some polymeric systems and to have no effect in others.[54,55] Physical aging, on the other hand, is generally known to (slightly) decrease the relaxation strength of a sub-T_g relaxation. In our case, following a 60 days exposure to dry environment at 20 °C, we measured a decrease in $\Delta\epsilon_\beta$ of about 10^{-3}, a negligible change on the scale of Figure 10.

Although it is clear that moisture affects the local dynamics and that some details about the molecular origin of local relaxations can be gleaned from DRS, a great deal more can be learned about the nature of the network−water interactions from the FTIR spectra. Important unanswered questions are as follows: (1) in what form (single molecules, dimers, trimers, clusters) does water reside within the adhesive; (2) at what network sites does water form hydrogen bonds; (3) in how many hydrogen bonds does a water molecules participate? To facilitate visualization and interpretation of the relevant molecular-level events, we show in Figure 13 a schematic of a fragment of the network with absorbed water molecules. Possible network−water interactions are indicated by dashed lines.

A series of NIR spectra were taken at select time intervals during exposure to the environment. Difference spectra were then obtained by subtracting the spectrum of a dry network from that of each wet network and are displayed in Figure 14. Water uptake causes pronounced changes in the 4950−5400 and 6200−7500 cm^{-1} ranges. The increase in the intensity of absorption in the 4950−5400 cm^{-1} range has been associated with the combination of asymmetric stretching (ν_3) and bending deformation (ν_2). Since hydrogen bonding has the opposite effect on stretching and bending vibrations, it is difficult to provide a molecular interpretation of the effect of moisture on the combination mode, and no further attempts were made along those lines. Instead, attempts were made to quantify the absorption range of 6200−7500 cm^{-1}, which is attributed to hydroxyl vibrations. Deconvolution of the difference spectra reveals the presence of three absorption bands in that range, centered at 7085, 6834, and 6541 cm^{-1}, respectively. As an example we show, in the inset of Figure 14, a deconvoluted difference spectrum for a sample containing 0.46% moisture. Similar spectra were recorded for other systems that range from the liquid mixtures of water with polar and nonpolar solvents to cross-linked thermoset networks.[56−59] The key question regards the interactions that underlie those three deconvoluted peaks and an explanation is offered by postulating the existence of three spectroscopically distinguishable forms of hydrogen bonding, termed S_0, S_1, and S_2, where subscripts zero, one and two denote the number of hydrogen atoms of a water molecule that participate in hydrogen bonding. We note that hydrogen bonding via water oxygen is possible but is not recorded by this method. On the basis of the changes in the breadth and the full width at half-height (fwhh) of the peaks at 7085, 6834, and 6541 cm^{-1}, an argument was put forward to associate those absorption bands with S_0, S_1, and S_2 forms, respectively. Once those assignments were made, we proceeded to calculate the relative contribution (%) of each form of hydrogen bonding, S_i, (where $i = 0, 1, 2$) and the ratio of hydrogen bonded to the total absorbed water, S_t (where $S_t = S_0 + S_1 + S_2$). It is assumed that S_i/S_t is proportional to C_i/C_t, where C is the concentration given as $C = A/a$, A is the area under the absorption peak and a is the absorption coefficient. As a first approximation, the literature values[56] of absorption coefficients a_0, a_1, and a_2 were used for S_0, S_1, and S_2 forms, respectively. Equation 3 was then used to calculate the relative concentration of each species:

$$\frac{C_i}{C_t} = \frac{S_i}{S_t} = \frac{A_i/a_i}{A_{7085}/a_0 + A_{6834}/a_1 + A_{6541}/a_2} \qquad (3)$$

The relative ratio of various forms of absorbed water is plotted as a function of water content in Figure 15. It is interesting to note that about 30% of the absorbed water is in the S_0 form, 50% in the S_1 form, and 20% in the S_2 form. Note also that the ratio of any absorbed species (S_i) to the total absorbed water (S_t) varies little with moisture content (%). We reiterate that the S_0 form represents a water molecule that does not form hydro-

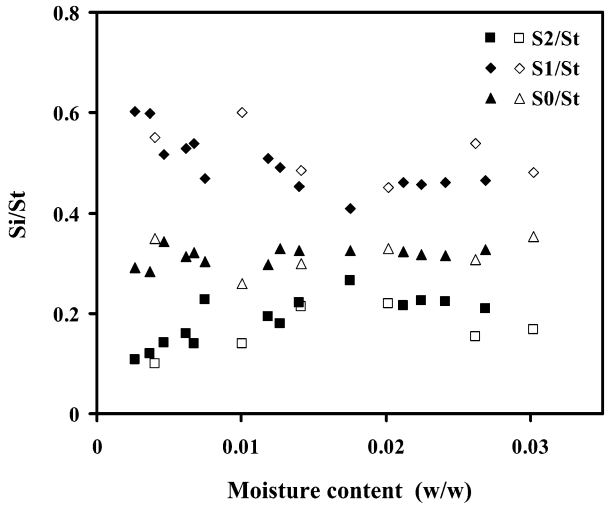

Figure 15. Relative ratio of the three forms of absorbed water (S_0, S_1, and S_2) to the total water content (S_t) as a function of moisture content. Solid symbols represent NIR results, open symbols the results from molecular simulations.

gen bonds through either of its hydrogen atoms but can do so through its oxygen atom. We also acknowledge the work by Weir et al., who used UV reflection spectroscopy to study water−epoxy interactions, though their method was limited to the detection of water−SO_2 interactions.[60]

Finally, molecular simulations were conducted in order to provide additional molecular level insight into the water−network interactions in our systems. In recent years, simulation studies have revealed interesting information about molecular structure of water and adhesives. Examples include, but are not limited to, the studies of the dynamics of pure water, [61,62]crystallization of water,[63] molecular dynamics of water−polymer solutions,[64] simulations of structure and properties of cross-linked resins,[65] and molecular dynamics of tethered chains in polymer melt adhesives.[66] Here, however, we report for the first time a molecular simulation study of hydrogen-bonded states of water molecules absorbed in a thermoset network adhesive. For more detailed description of our procedure the reader is referred to the experimental part; in sum, however, the amorphous cell containing a stoichiometric DGEBA−DETA network together with a select number of water molecules was subjected to a thermal history that parallels the experimental conditions and the final structure was recorded and studied. A hydrogen bond count was conducted based upon two criteria: [67] (1) the distance between the proton and the acceptor is shorter than 2.4 Å, and (2) the donor-proton-acceptor angle is greater than 145°. Our principal findings are as follows. It was established that a water molecule could (1) form a hydrogen bond with hydroxyl oxygen, ether oxygen, and/or tertiary amine nitrogen of the polymer network, (2) form a hydrogen bond with another water oxygen, and (3) act as a hydrogen bond acceptor for hydroxyl hydrogen of the polymer network. The majority of absorbed water molecules reside in the network as single molecules, and that is true at all levels of water content. Dimers are first found at the water content of 0.4% (by weight); trimers appear at about 1.4% and clusters of four water molecules at above 2.0%. A larger cluster (involving six water molecules) was found only once in over 70 simulations. We emphasize that in the trimers and clusters observed in our study, water molecules were

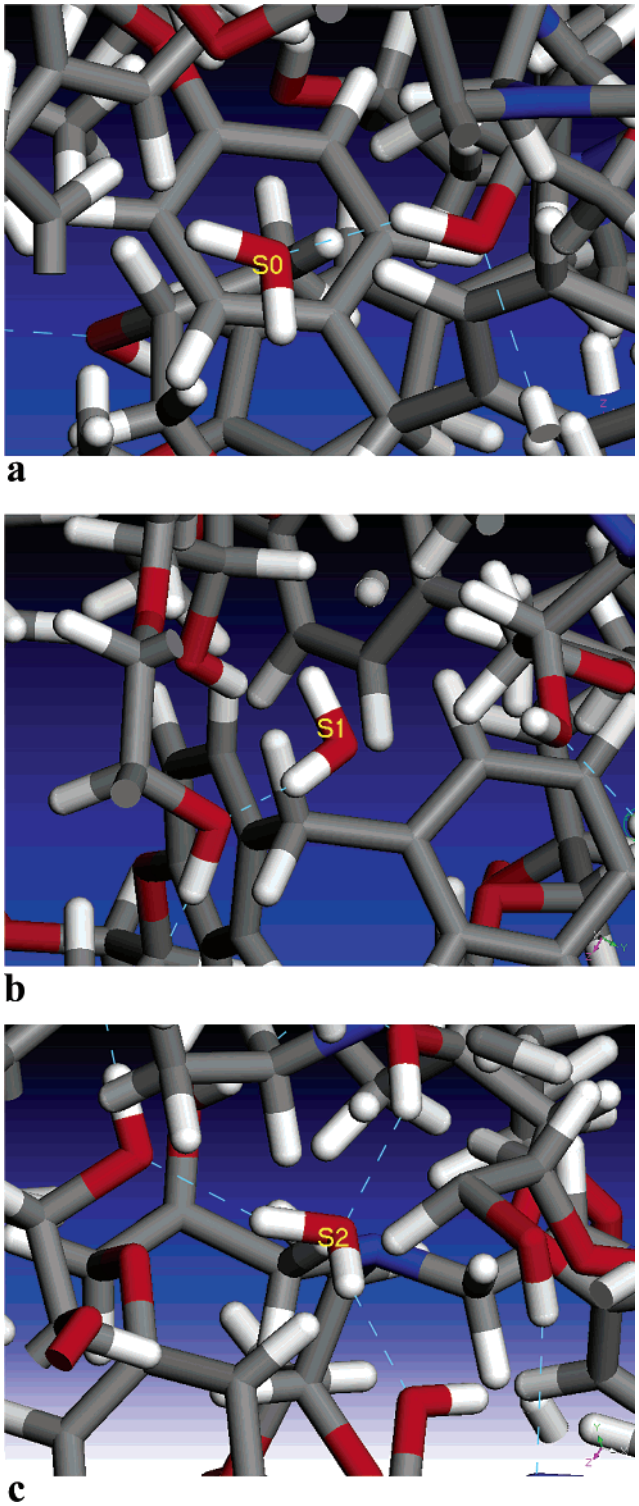

Figure 16. Snapshots from the results of molecular simulations showing three different forms of water molecules in the network: (a) the S_0 form; (b) the S_1 form; (c) the S_2 form.

linked through hydrogen bonds but did not necessarily form cyclic structures that have been reported in the simulation studies of liquid water.[68] Of all S_0 molecules, about two-thirds formed hydrogen bonds through the oxygen atom. If the one-third of S_0 molecules that did not form hydrogen bonds are considered as "free water" then its total amount stands at about 10%. That number is larger than the estimate obtained from the DRS data (ca. 5%), but considering the assumptions involved and

the precision limit of the measurements, the observed agreement is excellent.

The images of S_0, S_1, and S_2 forms generated by simulation are illustrated in Figure 16, in which hydrogen bonds appear as dashed lines. Figure 16a shows an example of the S_0 water molecule located in the center of the figure (oxygen is red, hydrogens are white). Note that neither of its hydrogens forms a hydrogen bond with the network, while its oxygen bonds to the hydroxyl group of the network. Figure 16b shows an example of the S_1 form; here, the water molecule in the center of the figure forms one hydrogen bond, in this case with the hydroxyl oxygen of the glycidyl group. Figure 16c shows an example of the S_2 form in which both hydrogens form bonds with the network.

The results obtained from molecular simulations were quantified and used to calculate the relative contribution (%) of each form of hydrogen bonding, S_i, (where $i = 0, 1, 2$) and the ratio of hydrogen bonded to the total absorbed water, S_t (where $S_t = S_0 + S_1 + S_2$). A comparison of the NIR results with the results from molecular simulations is illustrated in Figure 15. The observed agreement between the two techniques regarding the relative contribution of each form of hydrogen bonding is excellent.

IV. Conclusions

We have completed an investigation of the interactions between absorbed moisture and a glassy polymer network using DRS, NIR, and molecular simulations. The results of this study provide new insight into the local molecular dynamics and the chemical interactions between the polymer network and the absorbed water. The intensity and the dielectric relaxation strength of the local processes (β and γ) increase with moisture uptake. In the moist networks, both processes are Arrhenius-like, with an activation energy of about 58 kJ/mol. The molecular origin of the β process is associated with the hydroxyl groups while the γ process involves the ether groups of the glycidyl moiety. NIR analysis revealed the presence of non-hydrogen-bonded and hydrogen-bonded water. Deconvolution of the NIR spectra yielded three spectroscopically distinguishable forms of hydrogen-bonded water, termed S_0, S_1, and S_2, where subscripts zero, one and two denote the number of hydrogen atoms of a water molecule that participate in hydrogen bonding. The non hydrogen-bonded water, termed S_0, is represented by the NIR absorption at 7085 cm^{-1}. The absorption bands at 6834 and 6541 cm^{-1} were assigned to the S_1 and S_2 forms, respectively. The relative contribution (%) of each form of hydrogen-bonded water, S_i, (where $i = 0, 1, 2$) and the ratio of hydrogen bonded to the total absorbed water, S_t (where $S_t = S_0 + S_1 + S_2$) were calculated from the NIR data and from the results of molecular simulations. The observed agreement between those two techniques was excellent.

Acknowledgment. This material is based on work supported by the AFOSR Polymer Matrix Composites Program (Contract No. F49620-01-1-0320, Dr. Charles Y.-C. Lee, Program Director).

References and Notes

(1) Jelinski, L. W.; Dumais, J. J.; Stark, R. E.; Ellis, T. S.; Karasz, F. E. *Macromolecules* **1983**, *16*, 1019.
(2) Maxwell, I. D.; Pethrick, R. A. *J. Appl. Polym. Sci.* **1983**, *28*, 2363.
(3) Jelinski, L. W.; Dumais, J. J.; Chiolli, A. L.; Ellis, T. S.; Karasz, F. E. *Macromolecules* **1985**, *18*, 1091.
(4) Aldrich, P. D.; Thurow, S. K.; McKennon; M. J.; Lyssy, M. E. *Polymer* **1987**, *28*, 2289.
(5) Nairn, B. J.; Dickstein, P. A.; Plausinis, D. J.; Spelt, J. K. *J. Adhes.* **1995**, *48*, 121.
(6) Pethrick, R. A.; Hollins, E. A.; McEwan, I.; MacKinnon, A. J.; Hayward, D.; Cannon, L. A. *Macromolecules* **1996**, *29*, 5208.
(7) Colombini, D.; Martinez-Vega, J. J.; Merle, G. *Polymer* **2002**, *43*, 4479.
(8) A strong initiative has emerged in recent years aimed at identifying and monitoring the underlying chemistry and physics on the *molecular level*. The most recent discussion meeting on this subject was held during the Annual Review of the AFOSR Polymer Matrix Composites Program (Dr. Charles Y.-C. Lee, Program Director), Long Beach, CA, May 11−12, 2002.
(9) Gledhill, R. A.; Kinloch, A. J. *J. Adhes.* **1974**, *6*, 315.
(10) Browning, C. E. *Polym. Eng. Sci.* **1978**, *18*, 16.
(11) Keenan, J. D.; Seferis, J. C.; Quinlivan, J. T. *J. Appl. Polym. Sci.* **1979**, *24*, 2375.
(12) Rowland, S. P., Ed. *Water in Polymers*; ACS Symposium Series 127; American Chemical Society: Washington, DC, 1980.
(13) Sedlacek, B.; Kahovec, J. Eds.; *Cross-linked Epoxies*; Walter de Gruyter: Berlin, 1987.
(14) Kaelble, D. H.; Moacanin, J.; Gupta, A. In *Epoxy Resins Chemistry and Technology*; May, C. A., Ed.; Marcel Dekker: New York, 1988; Chapter 6, p 603.
(15) Apicella, A. In *International Encyclopedia of Composites*; Lee, S. M., Ed.; VCH Publishers: New York, 1990; Vol. 2.
(16) de Neve, B.; Shanahan, M. E. R. *J. Adhes.* **1995**, *49*, 165.
(17) Maggana, C.; Pissis, P. *J. Polym. Sci., Part B: Polym. Phys.* **1999**, *37*, 1165.
(18) Soles, C. L.; Chang, F. T.; Gidley, D. W.; Yee, A. F. *J. Polym. Sci., Part B: Polym. Phys.* **2000**, *38*, 776.
(19) Affrossman, S.; Banks, W. M.; Hayward, D.; Pethrick, R. A. *Proc. Inst. Mech. Eng. Part C* **2000**, *214*, 87.
(20) Bao. L. R.; Yee, A. F.; Lee, C. Y.-C. *Polymer* **2001**, *42*, 7327.
(21) Williams, G. In *Keynote Lectures in Selected Topics of Polymer Science*; Riande, E., Ed.; CSIC: Madrid, 1997; Chapter 1, pp 1−40.
(22) Williams, G. In *Comprehensive Polymer Science*; Allen, G., Bevington, J. C., Eds.; Pergamon: Oxford, England, 1989; Vol. 2, Chapter 7, pp 601−632.
(23) Williams, G. In *Dielectric Spectroscopy of Polymeric Materials*; Runt, J. P., Fitzgerald, J. J., Eds.; American Chemical Society: Washington, DC, 1997; Chapter 1, pp 3−65.
(24) Kremer, F.; Schönhals, A. Eds.; *Broadband Dielectric Spectroscopy*, Springer-Verlag: Berlin, 2002.
(25) Fitz, B.; Andjelic, S.; Mijovic, J. *Macromolecules* **1997**, *30*, 5227.
(26) Mijovic, J.; Duan, Y.; Miura, N.; Monetta, T. *Polym. News* **2001**, *26*, 251.
(27) Kremer, F.; Schönhals, A. In *Broadband Dielectric Spectroscopy*; Kremer, F., Schönhals, A., Eds.; Springer-Verlag: Berlin, 2002; Chapter 2, pp 35−57.
(28) Kranbuehl, D. In *Dielectric Spectroscopy of Polymeric Materials*; Runt, J. P.; Fitzgerald, J. J., Eds.; American Chemical Society: Washington, DC, 1997;. Chapter 11, pp 303−328.
(29) Sun, H. *J. Phys. Chem. B* **1998**, *102*, 7338.
(30) Greengard, L.; Rokhlin, V. I. *J. Comput. Phys.* **1987**, *73*, 325.
(31) Schmidt, K. E.; Lee, M. A. *J. Stat. Phys.* **1991**, *63*, 1223.
(32) Ding, H. Q.; Karasawa, N.; Goddard, W. A. *J. Chem. Phys.* **1992**, *97*, 4309.
(33) Havriliak, S., Jr.; Negami, S. *Polymer* **1967**, *8*, 161.
(34) Williams, G.; Watts, D. C. *Trans. Faraday Soc.* **1970**, *66*, 80.
(35) Schroter, K.; Unger, R.; Reissig, S.; Garwe, F.; Kahle, S.; Beiner, M.; Donth, E. *Macromolecules* **1998**, *31*, 8966.
(36) Kudlik, A.; Benkhof, S.; Blochowicz, T.; Tschirwitz, C.; Rössler, E. *J. Mol. Struct.* **1999**, *479*, 201.
(37) Correia, N. T.; Ramos, J. J. M. *Phys. Chem. Chem. Phys.* **2000**, *2*, 5712.
(38) Döss, A.; Paluch, M.; Sillescu, H.; Hinze, G. *Phys. Rev. Lett.* **2002**, *88*, 095701.
(39) Ngai, K. L. *J. Chem. Phys.* **1998**, *109*, 6982.
(40) Johari, G. P.; Goldstein, M. *J. Chem. Phys.* **1970**, *53*, 2372.
(41) Pochan, J. M.; Gruber, R. J.; Pochan, D. F. *J. Polym. Sci., Polym. Phys. Ed.* **1981**, *19*, 143.

(42) Butta, E.; Livi, A.; Levita, G.; Rolla, P. A. *J. Polym. Sci., Part B: Polym. Phys.* **1995**, *33*, 2253.
(43) Mijovic, J.; Andjelic, S. *Macromolecules* **1995**, *28*, 2787.
(44) Socrates, G. *Infrared Characteristic Group Frequencies, Tables and Charts*, 2nd ed.; John Wiley & Sons: Chichester, England, 1994; p 69.
(45) Frisch, H. L. *Polym. Eng. Sci.* **1980**, *20*, 1.
(46) Mikols, W. J.; Seferis, J. C.; Apicella, A.; Nicolais, L. *Polym. Comp.* **1982**, *3*, 118.
(47) Apicella, A.; Nicolais, L.; de Cataldis, C. *Adv. Polym. Sci.* **1985**, *66*, 189.
(48) Grave, C.; McEwan, I.; Pethrick, R. A. *J. Appl. Polym. Sci.* **1998**, *69*, 2369.
(49) Sato, T.; Chiba, A.; Nozaki, R. *J. Chem. Phys.* **1999**, *110*, 2508.
(50) Barthel, J.; Bachhuber, K.; Buchner, R.; Hetzenauer, H. *Chem. Phys. Lett.* **1990**, *165*, 369.
(51) Extrapolated from the data in: Okada, K.; Yao, M.; Hiejima, Y.; Kohno, H.; Kajihara, Y. *J. Chem. Phys.* **1999**, *110*, 3026.
(52) Auty, R. P.; Cole, R. H. *J. Chem. Phys.* **1952**, *20*, 1309.
(53) Mijovic, J.; Miura, N.; Zhang, H.; Duan, Y. *J. Adhes.* **2001**, *77*, 323.
(54) Fischer, E. W.; Hellmann, G. P.; Spiess, H. W.; Hörth, F. J.; Ecarius, U.; Wehrle, M. *Makromol. Chem. Suppl.* **1985**, *12*, 189.
(55) Floudas, G.; Fytas, G.; Fischer, E. W. *Macromolecules* **1991**, *24*, 1955.
(56) Choppin, G. R.; Violante, M. R. *J. Chem. Phys.* **1972**, *56*, 5890 and references therein.
(57) Musto, P.; Ragosta, G.; Mascia, L. *Chem. Mater.* **2000**, *12*, 1331.
(58) Cotugno, S.; Larobina, D.; Mensitieri, G.; Musto, P.; Ragosta, G. *Polymer* **2001**, *42*, 6431.
(59) Musto, P.; Ragosta, G.; Scarinzi, G.; Mascia, L. *J. Polym. Sci., Part B: Polym. Phys.* **2002**, *40*, 922.
(60) Weir, M. D.; Bastide, C.; Sung, C. S. P. *Macromolecules*, **2001**, *34*, 4923.
(61) Starr, F. W.; Nielsen, J. K.; Stanley, H. E. *Phys. Rev. Lett.* **1999**, *82*, 2294.
(62) Shpakov, V. P.; Roger, P. M.; Tse, J. S.; Klug, D. D.; Belosludov, V. R. *Phys. Rev. Lett.* **2002**, *88*, 155502−1.
(63) Matsumoto, M.; Saito, S.; Ohmine, I. *Nature* **2002**, *416*, 409.
(64) Smith, G. D.; Bedrov, D. *Macromolecules* **2002**, *35*, 5712.
(65) Yarovsky, I.; Evans, E. *Polymer*, **2002**, *43*, 963.
(66) Sides, S. W.; Grest, G. S.; Stevens, M. J. *Macromolecules*, **2002**, *35*, 566.
(67) Berndt, K. D.; Güntert, P.; Wüthrich, K. *J. Mol. Biol.* **1993**, *234*, 735.
(68) Ludwig, R. *Angew. Chem., Int. Ed.* **2001**, *40*, 1808 and references therein.

MA021568Q